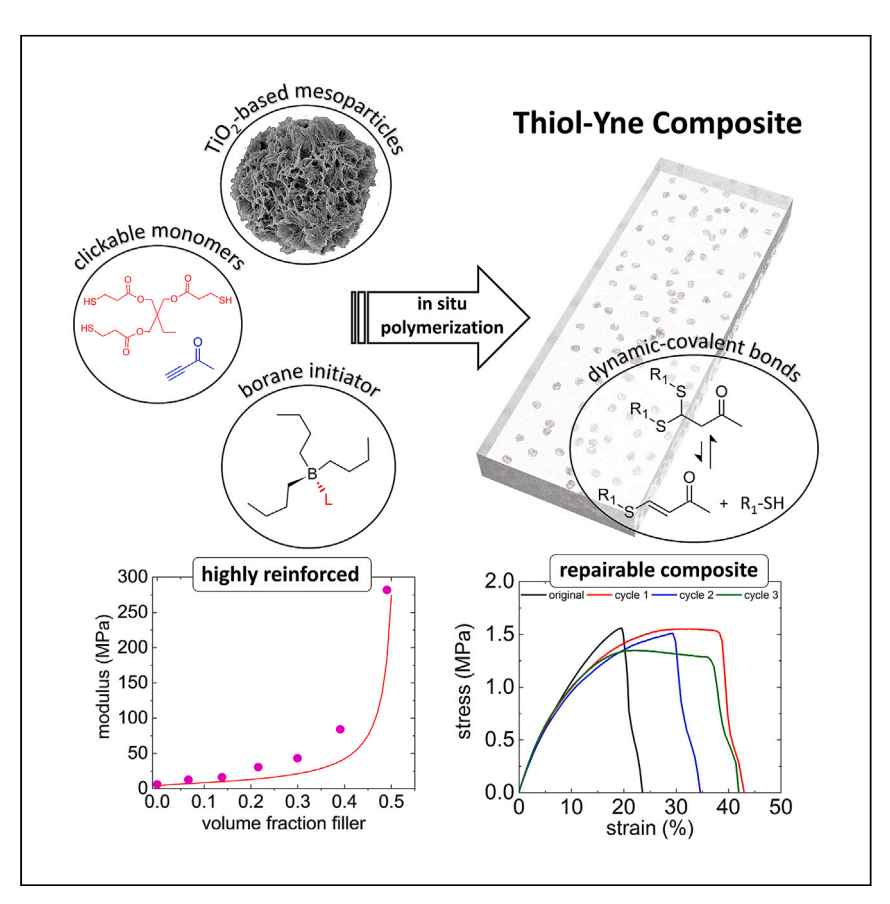


Article

Repairable reinforced composites of 1D TiO₂ lepidocrocite mesoparticles and thiol-yne click networks via alkylborane-initiated *in situ* polymerization



Advanced composites with multifunctionality, scalable constituents, and morphological control remain a synthetic challenge often requiring sophisticated fabrication processes. Wilson et al. report a synthetic pathway to multifunctional composites from scalable, highly reinforcing titania mesoparticles and a reprocessable, cross-linked polymeric elastomer through a simple and robust processing route using "click" chemistry, *in situ* polymerization, dynamic covalent bonds, and a custom alkylborane initiator.

Olivia R. Wilson, Michael S. Carey, Jacob H. Cope, ..., Tarek A. ElMelegy, Michel W. Barsoum, Andrew J.D. Magenau

ajm496@drexel.edu

Highlights

Borane initiator drives bulk, *in situ* thiol-yne polymerization to high conversion

Dispersed, reinforcing mesoparticles enhance composite modulus by 47-fold

Dynamic-covalent thioacetal bonds enable composite repair over many damage cycles

Scalable TiO_2 mesoparticles assemble from 1D titania-based lepidocrocite nanofilaments

Wilson et al., Cell Reports Physical Science 4, 101434

June 21, 2023 © 2023 The Authors. https://doi.org/10.1016/j.xcrp.2023.101434





Article

Repairable reinforced composites of 1D TiO₂ lepidocrocite mesoparticles and thiol-yne click networks via alkylborane-initiated *in situ* polymerization

Olivia R. Wilson,¹ Michael S. Carey,¹ Jacob H. Cope,¹ Hussein O. Badr,¹ Jacob M. Nantz,¹ Tarek A. ElMelegy,¹ Michael W. Barsoum,¹ and Andrew J.D. Magenau^{1,2,3,*}

SUMMARY

Synthesizing high-performance, multifunctional composites often entails poor filler dispersion, complex processes, or limited processing conditions. Hence, the advent of versatile syntheses employing simple conditions, inexpensive fillers, standard equipment, and robust reactions could expand attainable composites having enhanced performance, functionality, and customizability. We report on the synthesis of a novel multifunctional elastomeric composite from a new, reinforcing titania-based filler and a repairable, dynamic-covalent thiol-yne network or dissociative covalent adaptable network. Composites were processed by in situ polymerization via thiol-yne "click" chemistry initiated with a trialkylborane. Composite processing yields quantitative monomer conversion and uniform filler dispersion. The filler was a titania-based mesoparticle, self-assembled from 1D lepidocrocite nanofilaments through a recently discovered, scalable, and nearly universal route to wideranging nanostructures. A 47-fold enhancement in the modulus was achieved with 60 wt % filler versus the neat polymer, agreeing with theory. The reinforced, cross-linked composites were multifunctional, providing reprocessability over multiple damage-repair cycles with restoration of their mechanical properties.

INTRODUCTION

High-performance and multifunctional composites, commonly achieved through multiscale architectures and judiciously selected constituents, have long been pursued for a wide range of advanced applications. ^{1,2} At present, though, their syntheses can be challenging and impractical, often times having poor filler dispersion, incompatible constituents, non-scalable fillers, and onerous fabrication processes. Thus, demand exists for the development of new synthetic pathways that can maintain a composite's high performance, multifunctionality, and microstructural control while also using constituents that are scalable, inexpensive, and versatile.

Quite recently, we discovered a simple, one-pot, highly-scalable, and nearly universal sol-gel-based process to convert water-insoluble transition metal carbides, nitrides, borides, silicides, and even economically advantageous oxides into a plethora of materials from sub-nanoscale nanofilaments to 2D flakes and meso-scopic particles.^{3–5} The common parameter in our process was the use of a high pH reaction system that initiates the bottom-up synthesis of these materials, which, to date, has been primarily mediated by quaternary ammonium bases, namely tetramethylammonium hydroxide. In one study, we immersed six different



¹Department of Materials Science and Engineering, Drexel University, Philadelphia, PA 19104, USA

²Twitter: @magenaugroup

³Lead contact

^{*}Correspondence: ajm496@drexel.edu https://doi.org/10.1016/j.xcrp.2023.101434





manganese precursors (e.g., Mn_3O_4) in tetramethylammonium hydroxide solutions under an ambient atmosphere and at mild temperatures ($50^{\circ}C-80^{\circ}C$) to yield flexible films of crystallized 2D birnessite flakes after mere washing and filtration.⁴

More germane to this work, we found that this process was equally effective with ten water-insoluble titanium precursors—TiC, TiN, TiB₂, etc.—causing their transformation into 1D titania-based lepidocrocite nanofilaments and higher-order structures. Such titania nanofilaments are new in that their Raman spectra resemble titania (TiO₂) lepidocrocite but differ in that their X-ray diffraction patterns are unlike any other known TiO₂-based material. So Continued investigation and density functional theory have since revealed that the 1D nanofilaments grow along the [100] plane with respective a and c lattice parameters of ca. 3.78 and 3.04 Å. The nanofilaments were also found to self-assemble in two directions, producing 2D flakes that stack along the [001] plane. More recently, we discovered that if the 1D nanofilaments were washed with LiCl to a neutral pH, their self-assembly occurs into free-flowing individual TiO₂-based lepidocrocite mesoparticles (MPs), which are the reinforcing phase used in this contribution and the subject of later discussion.

Beyond our process's versatility, the synthetic route to these nanostructures was also found to be pragmatic and scalable, advantageously utilizing aqueous media, mild temperatures, inexpensive reagents, and minimal purification while generating high yields at the 10–100 gram scale using nothing more sophisticated than a stir plate and a plastic reactor.^{3,4} While the prospects of these materials are largely unknown, preliminary reports have found them to possess promising properties for biomedical, electrocatalytic, and energy storage applications.^{3–5} At present, however, none of these materials have been used as constituents in any hybrid or composite material. Hence, we imagined that such readily generated materials could enable the exploration of highly filled composites without prohibitive cost and that their versatility would enable composite designs with wide-ranging morphological and compositional options for the filler phase.

While scalable and versatile fillers are essential for composite design, one must also carefully consider the matrix and compounding strategy to achieve multifunctionality and the desired microstructure in a composite. One valuable compounding route that offers excellent filler dispersibility, mild processing conditions, significant property enhancement, and access to both thermoplastics and thermosets is *in situ* polymerization. ^{6–10} To efficiently employ *in situ* polymerization, the underlying reaction should be robust, capable of tolerating a wide range of fillers and loadings while still ensuring proper matrix formation. One powerful class of reaction, "click" chemistry, embodies these attributes and is exemplified by its simple execution, modularity, high yields, limited side products, and orthogonality. ¹¹ Thus, click reactions, for which the Nobel Prize was just awarded, are ideal candidates for *in situ* polymerization and network formation, conceivable with any number of highly efficient reactions like azide-alkyne cycloaddition, ^{11–13} activated esterification, ^{14,15} Diels-Alder cycloaddition, ^{16,17} and thiol-ene/yne additions, ^{18–20} among others. ^{21,22}

Of these, thiol-yne click chemistry and, in particular, their networks have a number of notable features making them attractive as prospective composite matrices. ^{18,19} From a structure-property standpoint, for instance, thiol-yne networks (TYNs) provide high cross-link densities, uniform microstructures, and minimal shrinkage. ^{18,23} As demonstrated by Fairbanks et al., analogous networks synthesized via thiol-ene and thiol-yne polymerizations showed a 6-fold increase in the cross-link density with the TYNs, manifested in a significant rise in the glass-transition temperature

Article



and rubbery modulus. ²³ Moreover, TYNs provide uniformly cross-linked networks allowing for well-defined and tailorable properties/transitions ²⁴ and minimal shrinkage for mitigating internal stresses and dimensional integrity. ²⁵ From a performance standpoint, TYNs also can be synthesized to contain dynamic-covalent bonds, thus opening the door to reprocessable networks (commonly termed vitrimers or covalent adaptable networks), ^{26,27} unlike their classic thermosetting and elastomeric counterparts. Dynamic-covalent bonds in TYNs were recently realized through activated alkynes (i.e., alkynones), enabling reprocessability in thermosets/hydrogels after multiple damage-repair cycles. Surprisingly, such dynamic-covalent TYNs have never been investigated for the fabrication of reprocessable composites, and to our knowledge, non-reprocessable TYNs and composites have only been reported in a few instances involving cadmium selenide, gold, and silica nanoparticles for sensing, optics, and other applications. ^{28–31}

Hence, we envisioned that novel composites could be fabricated with high mechanical reinforcement and reprocessability by uniquely combining our newly discovered and scalable MPs with dynamic-covalent TYNs. Most thiol-yne materials, however, are synthesized using photocuring, which is problematic when light accessibility is restricted or obstructed. Thus, complementary modes of initiation (thermal, redox, chemical, etc.) have proven of value in such instances involving long-cure depths or opaque fillers, ^{32–35} the latter scenario being in effect with our MP filler. Therefore, we reasoned that borane-based initiators—a focus of our group ^{36–39}—could be a solution and function as a new initiation pathway for the synthesis of alkylborane-initiated thiol-yne networks (Al-TYNs) and thiol-yne composites (Al-TYCs). Our prior work has shown that such air-stable and chemically triggered alkylborane-amine complexes permit unimpeded initiation and composite synthesis even when using high concentrations of light-attenuating filler in related thiol-ene composites. ³⁸

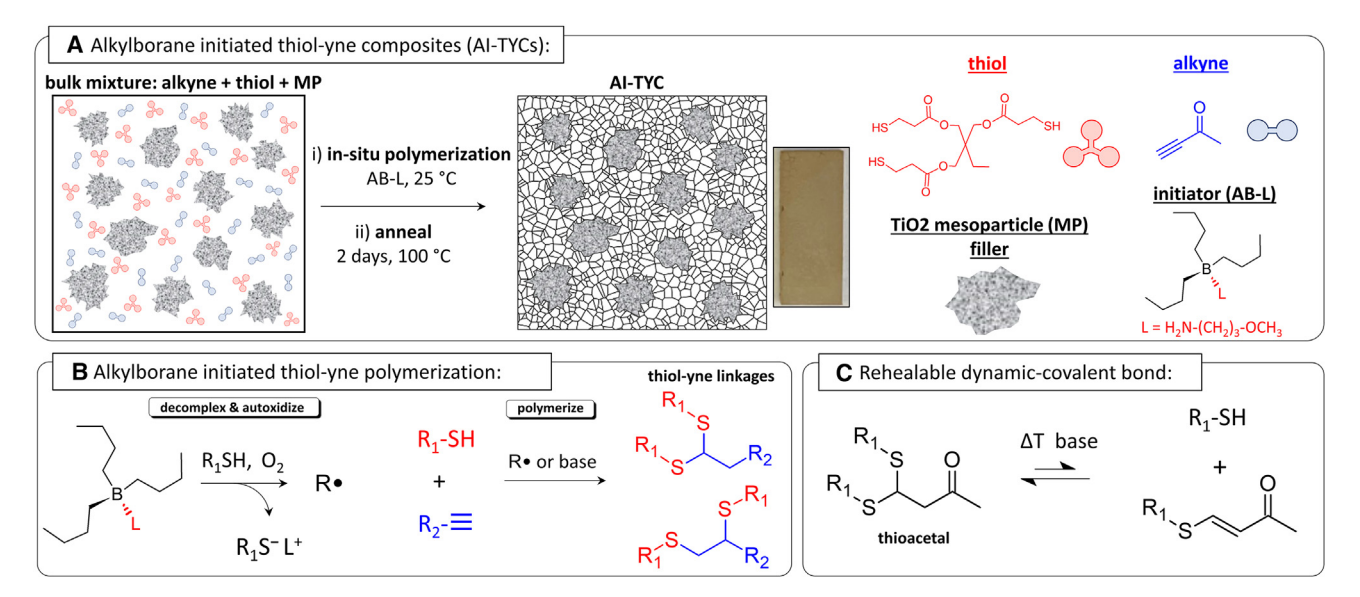
In this work, we investigate the efficacy of alkylborane initiation for synthesis of TYCs. The TiO_2 -based lepidocrocite MPs are chosen as the reinforcement because of their simple and scalable production, morphological versatility, and anticipated mechanical strength. As a proof of concept, Al-TYNs and Al-TYCs (20 wt % MPs) are synthesized through alkylborane initiation, and the extents of reaction are characterized, for which both systems achieve quantitative monomer conversion. To investigate structure-property relationships, a broader range of filler loadings are explored (10–60 wt %), and dynamic mechanical analysis of the resulting composites reveals a 47-fold increase in the storage modulus. Moreover, microscopy and X-ray diffraction confirm composite morphology and composition, respectively, and demonstrate that MPs are well dispersed throughout the polymer matrix. Finally, the Al-TYCs are subjected to three damage-repair cycles to demonstrate their repairability, which they achieve full mechanical recovery after each reprocessing event.

RESULTS AND DISCUSSION

Synthesizing TYCs with titania-based MPs

To achieve our goal, we elected to pursue an ambient condition and bulk *in situ* polymerization process (Scheme 1A) initiated by an alkylborane-ligand (AB-L) complex. *In situ* polymerization was conducted by first mixing the MP filler with two monomers, a difunctional alkyne (i.e., one alkyne reacts twice), and a trifunctional thiol to form a viscous monomer slurry. Bulk and room temperature conditions were targeted for ease of operation and to provide the necessary viscosity to stabilize MP dispersion and reduce sedimentation. Final composites were then obtained (see image in Scheme 1A) by triggering thiol-yne click polymerization by addition of the





Scheme 1. Synthesis of thiol-yne composites

(A) Synthesis of thiol-yne composites in bulk and ambient conditions using an alkylborane-amine initiator complex.

(B) Alkylborane mediated initiation and thiol-alkyne polymerization. (C) Network disassociation and dynamic bond exchange.

AB-L, i.e., tributylborane methoxypropylamine, followed by annealing. Upon addition of the initiator to the reaction, the AB-L decomplexes and autoxidizes, producing primary radicals (R·) and a thiolate/ammonium-ligand ion pair (R₁S⁻L⁺) (Scheme 1B) that drive the catalytic thiol-yne step-growth polymerization. Herein, polymerization occurs through a dual-initiation pathway involving both base-catalyzed and radical-catalyzed processes, thus forming both thioacetal and dithioether network linkages (Scheme 1B). Furthermore, our approach purposefully incorporates an activated alkyne monomer with an adjacent electron-withdrawing ketone since alkynone derived-TYNs produce dynamic-covalent bonds capable of network dissociation at elevated temperatures when in the presence of base (Scheme 1C).²⁷ To ensure dynamic-covalent character in our networks, our AB-L initiator was formulated to have a 20% molar excess of methoxypropylamine ligand, ensuring its availability for activating thioacetal bond dissociation and network repair.

The feasibility of our proposed synthesis was first examined by determining the extent of reaction after annealing both a neat AI-TYN and a 20 wt % AI-TYC. Both reactions were formulated with ca. 4 mol % AB-L and a ratio of [SH]: $[C \equiv CH] = 2:1$, which provided an equivalent number of reactive groups between the thiols and dual reactive alkynes. Fourier transform infrared (FTIR) analysis revealed that, in both cases, quantitative conversions were achieved (Figure 1A), evidenced by the complete disappearance of the alkyne bands at 3,254 and 2,090 cm⁻¹ from respective $C \equiv C$ and C-H stretches (blue boxes in Figure 1A) and the thiol stretching band at 2,570 cm⁻¹ (red box in Figure 1A). Importantly, this result highlights that alkylborane initiation and thiol-yne chemistry are unaffected by the presence of the MP filler. After annealing, the final materials were completely solid and flexible, with the AI-TYN having a dark maroon color and the AI-TYC having a brown clay-like color (Figure 1B). Additional experiments on unannealed AI-TYN samples revealed the necessity of the annealing step, showing complete disappearance of the alkyne but only $\sim 75\%$ conversion of the thiol (Figure S1), which is consistent with conversions reported in literature when using multifunctional thiols and photoinitiation.⁴⁰

Article



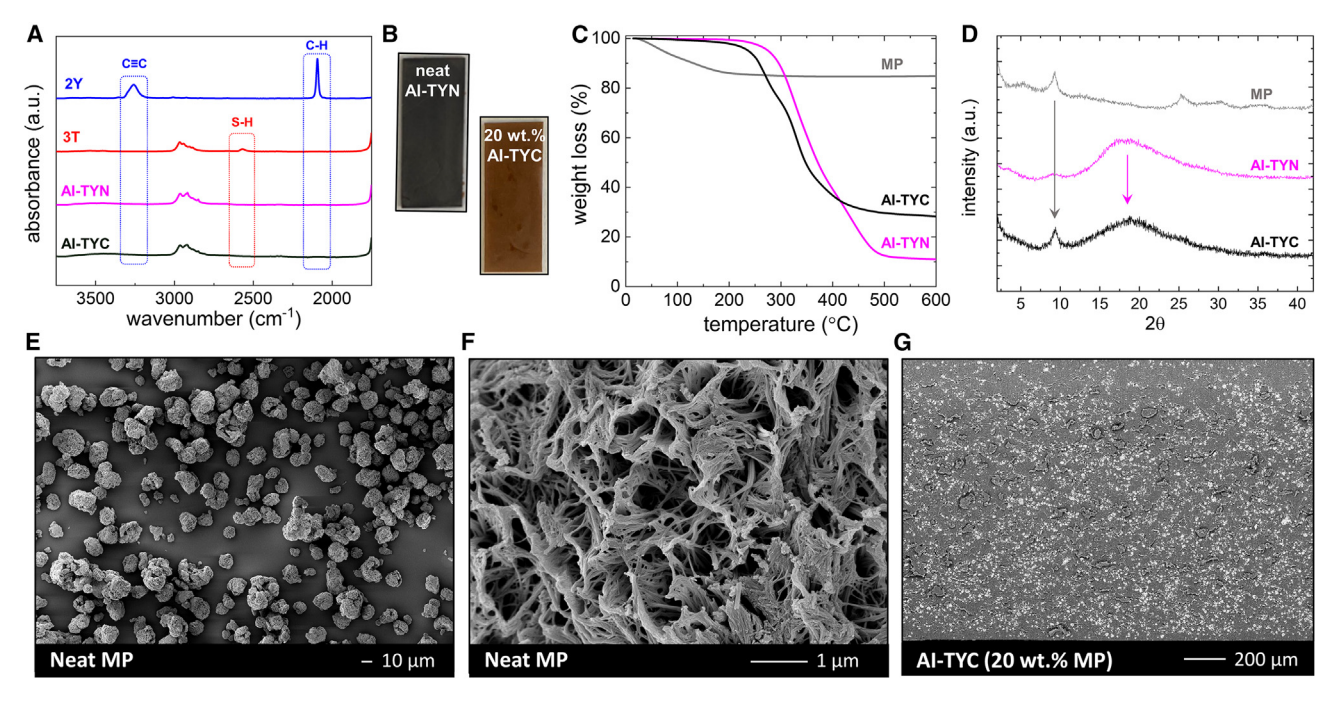


Figure 1. Characterization

- (A) FTIR spectra of the alkyne and thiol monomers and the resultant neat AI-TYN and 20 wt % MP AI-TYC.
- (B) Photographs of a neat AI-TYN and 20 wt % AI-TYC.
- (C) TGA in air of a neat MP, neat AI-TYN, and 20 wt % AI-TYC.
- (D) XRD patterns of the neat MP, neat AI-TYN, and 20 wt % AI-TYC.
- (E–G) SEM micrographs of the MPs (E and F) and 20 wt % reinforced AI-TYC (G).

As mentioned earlier, thiol-yne polymerization via an alkylborane-amine complex could reasonably occur through a base-catalyzed and/or radical-catalyzed mechanism. In the former case, primary amines, like our ligand (methoxypropylamine, pKa ≈ 9.8), 41 can deprotonate the propionate-based thiols on our trithiol monomer (pKa ≈ 9.3)⁴² to initiate the base-catalyzed process. In the latter case, initiating radicals can form by decomplexing the AB-L via ligand protonation followed by alkylborane autoxidation which drive the radical-catalyzed process. Radical generation is well known to occur after decomplexation of AB-L with amine-reactive compounds (acids, isocyanates, etc.), 36,43,44 and our previous work on thiol-ene networks shows that thiols alone are sufficient to initiate polymerization with alkylboranes.³⁸ Thus, to gain insight into the underlying mechanism, we conducted kinetic measurements using solely the amine ligand or uncomplexed alkylborane (Table S1) to determine which process occurred at a faster rate over a 30 min time frame (Table S1). These kinetic measurements suggest that under our conditions, both mechanisms are likely in operation, as the radical-catalyzed and base-catalyzed mechanisms occur at similar rates, i.e., 62% thiol conversion with alkylborane alone versus 58% with amine ligand alone. As a point of reference, our initiator complex with both alkylborane and amine achieved the highest thiol conversion at 73%. While further investigation is required to fully understand the extent and implications of each mechanism (such research efforts are ongoing), the goal of this contribution resides in the successful fabrication of novel, reinforced and repairable multifunctional composites using TYNs and our new titania-based lepidocrocite MPs.

After the successful synthesis of our first AI-TYC, we proceeded to evaluate the composite's loading, structure, and properties. The filler loading was confirmed



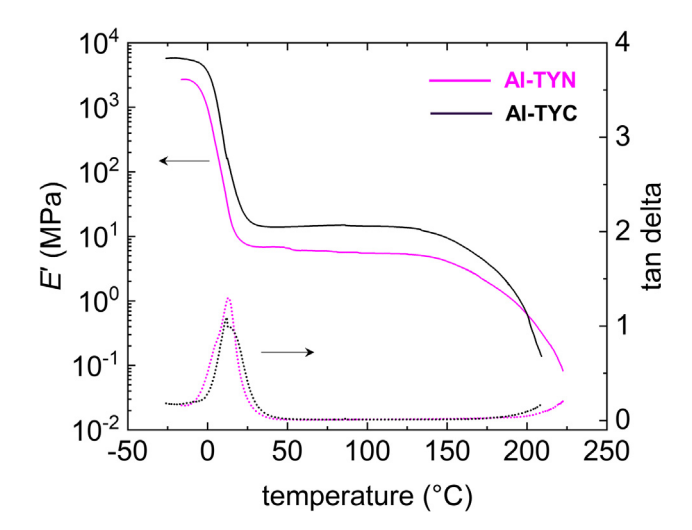


Figure 2. Dynamic mechanic analysisDMA temperature sweep of a neat AI-TYN and 20 wt % reinforced AI-TYC.

using thermogravimetric analysis (TGA) of the 20 wt % AI-TYC, neat network, and neat filler (Figure 1C). The MP alone maintained its original weight until \sim 600°C with the exception of a \sim 13% mass loss at lower temperatures due to residual solvents from purification. Conversely, the neat AI-TYN resulted in a char yield of \sim 12% with a maximum degradation rate occurring at \sim 327°C, aligning with literature values. Thus, by using the char yields of each component, we determined the composite's MP loading to be \sim 23 wt% (see supplemental information and Figure S2), which agrees well with the formulated amount of filler. Further analysis with X-ray diffraction (XRD) corroborated the presence of MP within our composite and that its structure was retained even after *in situ* polymerization and annealing. As shown in Figure 1D, the 20 wt% AI-TYC pattern portrayed the same characteristic signatures of each component, i.e., a low-angle diffraction peak at 20 \approx 9° from the MP and an amorphous halo from the TYN.

Scanning electron microscopy (SEM) was next employed to gain an understanding of the morphology and dispersion of filler within our composite by fracturing an AI-TYC sample and imaging its cross-section. The MP alone appeared as finite mesoscopic particles with diameters generally ranging from a few to tens of microns (Figure 1E), having a coral-like structure with a porous and cavernous morphology built from individual 1D nanofilaments (Figure 1F).³ Our highest-magnification SEM images (Figures S3G and S3H) clearly reveal the distinct and interconnected 1D nanofilaments that provide the underlying frame for each MP. Upon inspection of the composite, we observed that the MPs were well dispersed throughout the cross-section, appearing as lighter regions in the micrograph shown in Figure 1G, contrasting the featureless surface of the neat network (Figure S3). Dispersion of the MPs within the composite was further bolstered by energy-dispersive X-ray spectroscopy (EDS) SEM, which vividly showed elemental Ti signals from the MP filler distributed uniformly throughout the composite (Figure S4). Collectively, these results demonstrate that a good dispersion of MPs can be readily achieved through simple mechanical mixing and an in situ polymerization approach.

To better understand how this new filler impacted composite properties, dynamic mechanical analysis (DMA) was conducted on an AI-TYN and a 20 wt % AI-TYC. Specifically, the thermomechanical properties were assessed using a temperature

Article



sweep from ca. -25°C to 250°C (Figure 2), which we used as a preliminary tool to probe the effect of MPs on the composite's glass-transition temperature (T_a) , mechanical properties, and reprocessability. As anticipated, the neat network and composite were observed to have T_{as} below room temperature inferred from their peak $\tan \delta$ values, which affords their flexible characteristics. Unsurprisingly, even with a 20 wt % loading of MP, little difference (if any) in the T_a was observed between the neat AI-TYN (\sim 13°C) and the 20 wt % AI-TYC (\sim 14°C). Moreover, the temperature range of the T_g was found to be narrow, spanning only $\sim 20^{\circ}$ C, thus pointing toward the existence of a uniform network structure in both materials. In stark contrast to the T_{q} , a profound 2- to 3-fold increase in the storage modulus (E') was observed for the composite compared with the neat network ≤125°C (Figure 2), demonstrating a significant mechanical benefit from the MP filler. We attribute the enhanced E' to the filler's rigidity, its successful dispersion throughout the matrix, 45 and, uniquely, the infiltration of polymer into the open cavities of the MPs. In addition to mechanical reinforcement, the reprocessable nature of the network persisted in the composites, observed by the gradual decrease in E' at temperatures above ~125°C, similar to that of the neat AI-TYN. Such declining behavior in the rubbery plateau suggests an overall reduction in the cross-link density and the dissociative nature of the TYN.²⁷ Qualitatively, photographs of both materials after the temperature sweeps illustrate their ability to flow after being exposed to elevated temperatures (Figure S4).

Impact of filler loading on composite synthesis, structure, and performance

Intrigued by the notable enhancement in mechanical properties, we sought to better understand the influence of a broader range of MP loadings on the synthesis, structure, and mechanical performance of our Al-TYCs. Hence, we attempted to synthesize a series of composites using a larger range of loadings spanning from 10 to 60 wt % MP. To our surprise, we found that the *in situ* polymerization was quite tolerant to the MP loading, highlighting the robustness of alkylborane initiation and thiol-yne click chemistry. Across all the loadings, we observed a complete disappearance of the alkyne and thiol bands as determined by FTIR analysis (Figure S6), implying full monomer conversion in all instances. Moreover, our synthetic strategy gave predictable filler loadings, evidenced by the strong correlation between experimental and formulated amounts of filler (Figure 3A) from TGA, and consistently sub-ambient $T_{\rm g}$ s in all the composites, averaging around -2.5° C, according to differential scanning calorimetry (Figure S10).

Structural insights into the composites were next verified with XRD, providing both confirmation that the MP remained intact after processing, via persistence of the reflection at $2\theta \approx 9^{\circ}$, and evidence that the filler was distributed throughout matrix by the absence of any long-range order outside those inherent to the MPs (Figures 1D and S7). Further evidence of the morphology and filler dispersion was accomplished by cross-sectioning each AI-TYC film and imaging its fracture surface using a SEM (Figure 3B). Traversing from low to high loadings, a systematic increase in the MP content was clear, especially in the higher-magnification micrographs (Figure 3B), by the gradual uptick in the number of particulates. The MPs also appeared intimately mixed and in close contact with the network phase. From a larger vantage point, the lower magnification micrographs showed that the filler was quite well dispersed throughout the whole composite in all the AI-TYCs except for the 10 wt % composite. In this instance, a bias of filler was observed toward the bottom of the sample, which we attribute to sedimentation of the filler in the low-viscosity monomer slurry used during synthesis. In all other cases, higher loadings of MPs (>10 wt %) yielded suitably viscous monomer slurries that assisted in maintaining



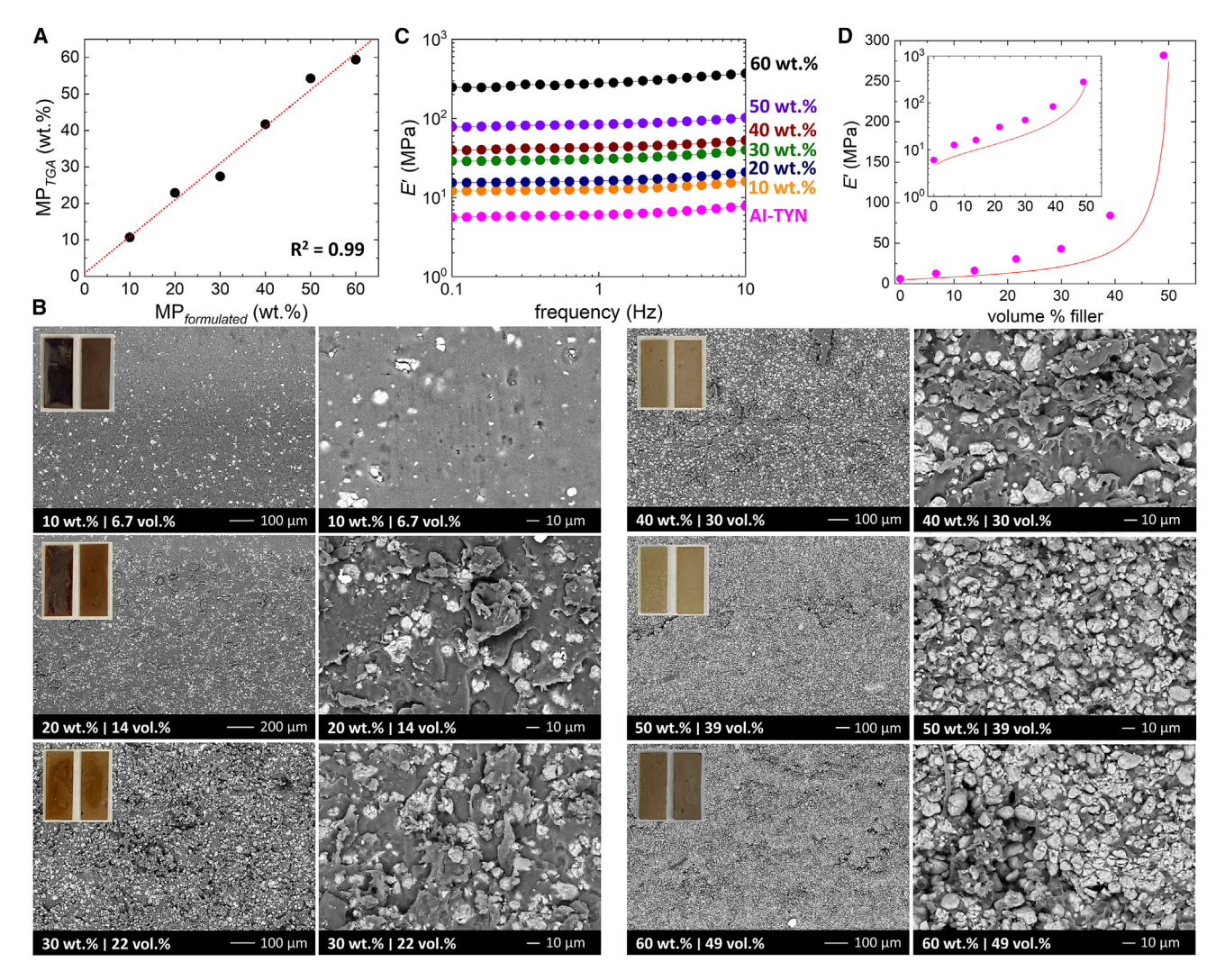


Figure 3. AI-TYCs with MP loadings of 10-60 wt %

- (A) Comparison of MP filler loading determined via TGA and formulated loadings.
- (B) Images of Al-TYC films and SEM micrographs of composite cross-sections as a function of filler loading. Insets show pictures of the composite films.
- (C) Composite storage moduli as a function of frequency over two decades at 25°C.
- (D) Dependence of composite storage modulus on filler loading. Numerical values for the modulus and loading are available in Table S2. Predictions of the storage modulus were made from a model of filled elastomers (see supplemental information section 2.8) shown in red. Inset shows the same results plotted on a semi-logarithmic plot.

the MP dispersion until network vitrification could occur. Additional EDS-SEM images in Figure S8 support our conclusions concerning the filler's dispersion.

After verifying the synthesis and morphology of our composites, we proceeded with mechanical characterization, uncovering how the MP loading impacted composite properties. Frequency sweeps conducted with DMA showed a progressive increase in E' as the loading of MP increased from 10 to 60 wt % (Figure 3C) and a frequency-independent modulus at all loadings indicative of a homogeneous and uniform polymer network. Strikingly, we found that the total improvement in the E' increased by 47-fold, from ca. 6 to 280 MPa, when comparing the neat AI-TYN with the 60 wt % AI-TYC, respectively (Figure 3C). To provide further insight, the wt % of filler was converted to vol % in Figure 3D using an experimentally determined MP density



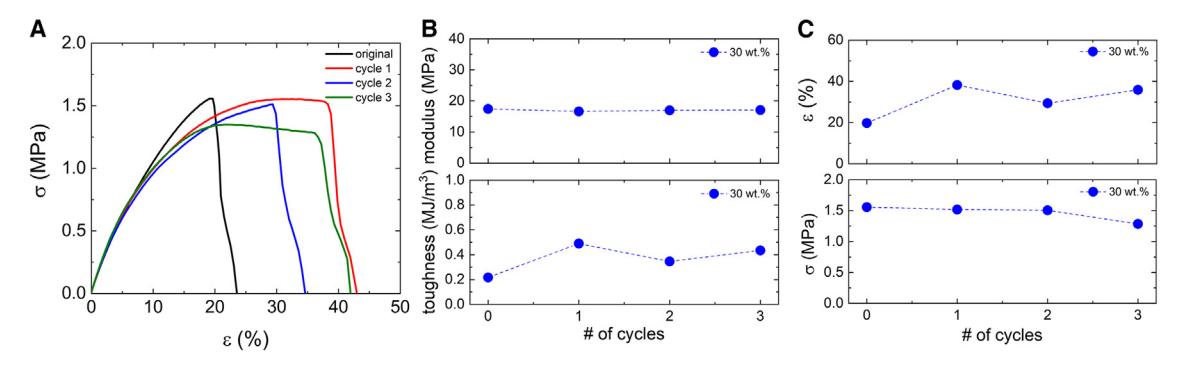


Figure 4. Repair via dynamic-covalent chemistry

(A) Stress-strain curves of a pristine and reprocessed 30 wt % composites after 3 damage-repair cycles during which the same sample was loaded in tension to failure and repaired by hot pressing the composite for 4 h under a pressure of 20 MPa at 100°C.

(B and C) Elastic modulus and toughness values (B) and strain at failure (ϵ) and stress at failure (σ) values (C) after each reprocessing cycle. All tensile tests were performed in ambient conditions.

of ~2 g/cm³ via geometric and gravimetric measurements (Figure S9). A more nuanced inspection of E' reveals that at lower loadings (MP \leq 30 vol %), the improvement in modulus was nearly linear but began to exhibit an exponentiallike enhancement at MP loadings ≥30 vol %. Breakaway from linearity appears to occur when the filler particles begin to contact themselves (see 50-60 wt % SEM images in Figure 3B), forming a percolation pathway and a brick-and-mortar morphology. Indeed, the accelerated enhancement in modulus becomes practically linear when plotted on a semi-logarithmic graph (Figure 3D, inset), providing a convenient tool for predicting composite properties. Theoretical models of concentrated elastomeric suspensions with spherical inclusions accurately describe our findings (red line in Figure 3D), giving further credence to our results, and predict a similar 47-fold enhancement in modulus as the system approaches conditions where the inclusions begin to touch. 46 Comparatively, in reference to a widely studied filler, this modulus enhancement is equivalent to the highest values ever reported for carbon nanotube composites. Moreover, even if compositionally different than our system (and not intrinsically repairable), low T_{α} elastomeric composites highly reinforced with hard spherical-like inclusions have shown comparable or lower modulus enhancements of \sim 17-fold using 110 nm silica spheres at \sim 40 vol % in a poly(diethylene glycol methacrylate) matrix, ⁴⁷ ~22-fold using 15–30 nm silica spheres at 45 vol % in an industrial acrylonitrile butadiene rubber, 48 and up to 60-fold using 20 μm radius polystyrene spheres at 45 vol % in a cross-linked poly(vinyl alcohol) matrix.⁴⁸ Importantly, our results demonstrate that these new and scalable fillers can be employed as highly effective mechanical reinforcers for elastomeric networks and, potentially, on a much broader scale with numerous other polymers.

Repair of TYCs via dynamic-covalent bond exchange

As a final evaluation of our composites, we sought to determine whether an MP based AI-TYC could be repaired by taking advantage of their dynamic-covalent bonds via the base-promoted reversible disassociation of the thioacetal bonds (Scheme 1C). Accordingly, we selected one AI-TYC with an intermediate loading, 30 wt % MP, and subjected it to multiple cycles of tensile testing to failure and then repair. To facilitate the repair mechanism, the AI-TYC was synthesized to contain residual base by using an AB-L initiator complex with a 20% molar excess of amine ligand. Thus, after tensile testing the original as-synthesized AI-TYC film to failure, the composite was then repaired via compression molding at 100°C



and 20 MPa for 4 h over three cycles. Figure 4A shows the resultant stress-strain curves of the original film and after each reprocessing step. Overall, the original and repaired stress-strain curves exhibited fairly consistent elastomeric behavior, with low stresses and high strains, characteristic of thiol-yne materials with subambient $T_{\rm g}$ s. Upon quantitative analysis, the reprocessed composites were observed to experience a slight improvement in toughness and strain at break, while the elastic modulus and stress at break remained largely unchanged (Figure 4B and 4C), indicating full restoration of the composite's mechanical integrity after each failure event. We speculate that any improvement in performance after reprocessing may be due to better integration of the constituents or formation of a more perfect network structure likely from further monomer/intermediate conversion or reconfiguration/relaxation of the network.

In summary, this contribution reports a new and robust synthesis of highly reinforced and repairable TYCs. Our synthetic approach entails an ambient condition and bulk in situ polymerization of thiol and alkyne monomers using an alkylborane-amine initiator complex while in the presence of a new mesoscopic particle self-assembled from 1D titania-based lepidocrocite nanofilaments. Alkylborane initiated thiol-yne polymerization was shown to be exceptionally tolerant to the MP filler content, achieving quantitative conversions in both neat networks and composites with up to 60 wt % filler. Through in situ polymerization, we found that the MP filler was remarkably well-dispersed within the polymer matrix in all cases except for the lowest filler loading. Impressively, we discovered that the incorporation of MP filler into the polymer network provides a significant mechanical reinforcement, amounting to a 47-fold enhancement in the composite's storage modulus. Moreover, even in the presence of 30 wt % filler, the matrix of the composites exhibited an excellent ability to repair itself, showing retained mechanical performance over three damage-repair cycles. We envision that the disclosed synthetic strategy may provide an avenue to new high performance and reprocessable composites for potential use in a range of advanced applications.

EXPERIMENTAL PROCEDURES

Resource availability

Lead contact

Further information and requests for resources should be directed to and will be fulfilled by the lead contact, Andrew Magenau (ajm496@drexel.edu)

Materials availability

The composites generated in this study can be made available upon reasonable request.

Data and code availability

The data generated in this study are included in the manuscript and supplemental information and will be made available upon reasonable request.

SUPPLEMENTAL INFORMATION

Supplemental information can be found online at https://doi.org/10.1016/j.xcrp. 2023.101434.

ACKNOWLEDGMENTS

A.J.D.M. would like to thank the American Chemical Society's Petroleum Research Fund (59903-DNI7) and Pennsylvania Manufacturing Innovation Program for partial

Article



support of this work. A.J.D.M. also thanks Callory Chemical (Pittsburgh, PA) for their generous donation of the alkylborane complex. M.W.B. thanks the National Science Foundation (DMR-2211319) for support of this work. The authors would like to thank Dr. Nicolas Alvarez and Dr. Christopher Li for the use of a planetary mixer, TGA, differential scanning calorimetry (DSC), and melt press.

AUTHOR CONTRIBUTIONS

A.J.D.M. and M.W.B. conceived and designed the presented work. O.R.W. led research and development, experimentation, and data analysis. M.S.C., J.H.C., H.O.C., J.M.N., and T.A.E. assisted in experimentation, data collection, and analysis. O.R.W., M.W.B., and A.J.D.M. drafted and wrote the manuscript. A.J.D.M. directed and coordinated the project.

DECLARATION OF INTERESTS

The authors declare no competing interests.

Received: February 6, 2023 Revised: May 3, 2023 Accepted: May 5, 2023 Published: May 31, 2023

REFERENCES

- Wegst, U.G.K., Bai, H., Saiz, E., Tomsia, A.P., and Ritchie, R.O. (2015). Bioinspired structural materials. Nat. Mater. 14, 23–36. https://doi. org/10.1038/nmat4089.
- Bai, H., Li, C., and Shi, G. (2011). Functional composite materials based on chemically converted graphene. Adv. Mater. 23, 1089– 1115. https://doi.org/10.1002/adma. 201003753.
- Badr, H.O., El-Melegy, T., Carey, M., Natu, V., Hassig, M.Q., Johnson, C., Qian, Q., Li, C.Y., Kushnir, K., Colin-Ulloa, E., et al. (2022). Bottom-up, scalable synthesis of anatase nanofilament-based two-dimensional titanium carbo-oxide flakes. Mater. Today 54, 8–17. https://doi.org/10.1016/j.mattod.2021.10.033.
- Badr, H.O., Montazeri, K., El-Melegy, T., Natu, V., Carey, M., Gawas, R., Phan, P., Qian, Q., Li, C.Y., Wiedwald, U., et al. (2022). Scalable, inexpensive, one-pot, facile synthesis of crystalline two-dimensional birnessite flakes. Matter 5, 2365–2381. https://doi.org/10.1016/j. matt.2022.05.038.
- Badr, H.O., Lagunas, F., Autrey, D.E., Cope, J., Kono, T., Torita, T., Klie, R.F., Hu, Y.-J., and Barsoum, M.W. (2023). On the structure of onedimensional TiO2 lepidocrocite. Matter 6, 128–141. https://doi.org/10.1016/j.matt.2022. 10.015.
- Byrne, M.T., and Gun'ko, Y.K. (2010). Recent advances in research on carbon nanotube– polymer composites. Adv. Mater. 22, 1672– 1688. https://doi.org/10.1002/adma. 200901545.
- Carey, M., Hinton, Z., Sokol, M., Alvarez, N.J., and Barsoum, M.W. (2019). Nylon-6/Ti3CZTz MXene nanocomposites synthesized by in situ ring opening polymerization of e-caprolactam and their water transport properties. ACS

- Appl. Mater. Interfaces 11, 20425–20436. https://doi.org/10.1021/acsami.9b05027.
- McDaniel, R.M., Carey, M.S., Wilson, O.R., Barsoum, M.W., and Magenau, A.J.D. (2021). Well-dispersed nanocomposites using covalently modified, multilayer, 2D titanium carbide (MXene) and in-situ "click" polymerization. Chem. Mater. 33, 1648–1656. https://doi.org/10.1021/acs.chemmater. 0c03972.
- Zou, H., Wu, S., and Shen, J. (2008). Polymer/ silica nanocomposites: preparation, characterization, properties, and applications. Chem. Rev. 108, 3893–3957. https://doi.org/10. 1021/cr068035a.
- Althues, H., Henle, J., and Kaskel, S. (2007). Functional inorganic nanofillers for transparent polymers. Chem. Soc. Rev. 36, 1454–1465. https://doi.org/10.1039/B608177K.
- Kolb, H.C., Finn, M.G., and Sharpless, K.B. (2001). Click chemistry: diverse chemical function from a few good reactions. Angew. Chem. Int. Ed. 40, 2004–2021. 2-5. https://doi. org/10.1002/1521-3773(20010601)40:11% 3C2004::AID-ANIE2004%3E3.0.CO.
- Magenau, A.J.D., Martinez-Castro, N., Savin, D.A., and Storey, R.F. (2009). Polyisobutylene RAFT CTA by a click chemistry site transformation approach: synthesis of poly(isobutylene-b-N-isopropylacrylamide). Macromolecules 42, 8044–8051. https://doi. org/10.1021/ma901685p.
- Martinez-Castro, N., Magenau, A.J.D., and Storey, R.F. (2010). Functional polyisobutylenes via a click chemistry approach. J. Polym. Sci. A. Polym. Chem. 48, 2533–2545. https://doi.org/ 10.1002/pola.24029.
- 14. Das, A., and Theato, P. (2016). Activated ester containing polymers: opportunities and

- challenges for the design of functional macromolecules. Chem. Rev. 116, 1434–1495. https://doi.org/10.1021/acs.chemrev.5b00291.
- Weaver, J.A., Morelly, S.L., Alvarez, N.J., and Magenau, A.J.D. (2018). Grafting-through ROMP for gels with tailorable moduli and crosslink densities. Polym. Chem. 9, 5173–5178. https://doi.org/10.1039/C8PY01324A.
- Delaittre, G., Guimard, N.K., and Barner-Kowollik, C. (2015). Cycloadditions in modern polymer chemistry. Acc. Chem. Res. 48, 1296– 1307. https://doi.org/10.1021/acs.accounts. 5b00075.
- Tasdelen, M.A. (2011). Diels-Alder "click" reactions: recent applications in polymer and material science. Polym. Chem. 2, 2133–2145. https://doi.org/10.1039/c1py00041a.
- Lowe, A.B., Hoyle, C.E., and Bowman, C.N. (2010). Thiol-yne click chemistry: a powerful and versatile methodology for materials synthesis. J. Mater. Chem. 20, 4745–4750. https://doi.org/10.1039/B917102A.
- Hoyle, C.E., Lowe, A.B., and Bowman, C.N. (2010). Thiol-click chemistry: a multifaceted toolbox for small molecule and polymer synthesis. Chem. Soc. Rev. 39, 1355–1387. https://doi.org/10.1039/b901979k.
- Magenau, A.J.D., Chan, J.W., Hoyle, C.E., and Storey, R.F. (2010). Facile polyisobutylene functionalization via thiol-ene click chemistry. Polym. Chem. 1, 831–833. https://doi.org/10. 1039/C0PY00094A.
- Blasco, E., Sims, M.B., Goldmann, A.S., Sumerlin, B.S., and Barner-Kowollik, C. (2017). 50th anniversary perspective: polymer functionalization. Macromolecules 50, 5215– 5252. https://doi.org/10.1021/acs.macromol. 7b00465.



Cell Reports Physical Science Article

- Howe, D.H., McDaniel, R.M., and Magenau, A.J.D. (2017). From click chemistry to crosscoupling: designer polymers from one efficient reaction. Macromolecules 50, 8010–8018. https://doi.org/10.1021/acs.macromol. 7b02041.
- Fairbanks, B.D., Scott, T.F., Kloxin, C.J., Anseth, K.S., and Bowman, C.N. (2009). Thiol—Yne photopolymerizations: novel mechanism, kinetics, and step-growth formation of highly cross-linked networks. Macromolecules 42, 211–217. https://doi.org/10.1021/ma801903w.
- Chan, J.W., Zhou, H., Hoyle, C.E., and Lowe, A.B. (2009). Photopolymerization of thiolalkynes: polysulfide networks. Chem. Mater. 21, 1579–1585. https://doi.org/10.1021/ cm803262p.
- Park, H.Y., Kloxin, C.J., Scott, T.F., and Bowman, C.N. (2010). Stress relaxation by Addition—Fragmentation chain transfer in highly cross-linked Thiol—Yne networks. Macromolecules 43, 10188–10190. https://doi. org/10.1021/ma1020209.
- Fan, B., Zhang, K., Liu, Q., and Eelkema, R. (2020). Self-healing injectable polymer hydrogel via dynamic thiol-alkynone double addition cross-links. ACS Macro Lett. 9, 776–780. https://doi.org/10.1021/acsmacrolett.0c00241.
- Van Herck, N., Maes, D., Unal, K., Guerre, M., Winne, J.M., and Du Prez, F.E. (2020). Covalent adaptable networks with tunable exchange rates based on reversible thiol-yne crosslinking. Angew. Chem. Int. Ed. 59, 3609–3617. https://doi.org/10.1002/anie.201912902.
- Stewart, M.H., Susumu, K., Oh, E., Brown, C.G., McClain, C.C., Gorzkowski, E.P., and Boyd, D.A. (2018). Fabrication of photoluminescent quantum dot thiol-yne nanocomposites via thermal curing or photopolymerization. ACS Omega 3, 3314–3320. https://doi.org/10.1021/ acsomega.8b00319.
- Boyd, D.A., Bezares, F.J., Pacardo, D.B., Ukaegbu, M., Hosten, C., and Ligler, F.S. (2014). Small-Molecule detection in thiol-yne nanocomposites via surface-enhanced Raman spectroscopy. Anal. Chem. 86, 12315–12320. https://doi.org/10.1021/ac503607b.
- Boyd, D.A., Naciri, J., Fontana, J., Pacardo, D.B., Shields, A.R., Verbarg, J., Spillmann, C.M., and Ligler, F.S. (2014). Facile fabrication of color tunable film and fiber nanocomposites via thiol click chemistry. Macromolecules 47, 695–704. https://doi.org/10.1021/ma401636e.

- Mitsube, K., Nishimura, Y., Nagaya, K., Takayama, S., and Tomita, Y. (2014).
 Holographic nanoparticle-polymer composites based on radical-mediated thiol-yne photopolymerizations: characterization and shift-multiplexed holographic digital data page storage. Opt. Mater. Express 4, 982–996. https://doi.org/10.1364/OME.4.000982.
- Garra, P., Dietlin, C., Morlet-Savary, F., Dumur, F., Gigmes, D., Fouassier, J.-P., and Lalevée, J. (2017). Photopolymerization processes of thick films and in shadow areas: a review for the access to composites. Polym. Chem. 8, 7088– 7101. https://doi.org/10.1039/C7PY01778B.
- Cole, M.A., Jankousky, K.C., and Bowman, C.N. (2013). Redox initiation of bulk thiol-ene polymerizations. Polym. Chem. 4, 1167–1175. https://doi.org/10.1039/C2PY20843A.
- Bowman, C.N., and Kloxin, C.J. (2008). Toward an enhanced understanding and implementation of photopolymerization reactions. AIChE J. 54, 2775–2795. https://doi. org/10.1002/aic.11678.
- Ye, S., Cramer, N.B., Stevens, B.E., Sani, R.L., and Bowman, C.N. (2011). Induction curing of thiol–acrylate and thiol–ene composite systems. Macromolecules 44, 4988–4996. https://doi.org/10.1021/ma200098e.
- Wilson, O.R., and Magenau, A.J.D. (2018). Oxygen tolerant and room temperature RAFT through alkylborane initiation. ACS Macro Lett. 7, 370–375. https://doi.org/10.1021/ acsmacrolett.8b00076.
- Timmins, R.L., Wilson, O.R., and Magenau, A.J.D. (2020). Arm-first star-polymer synthesis in one-pot via alkylborane-initiated RAFT. J. Polym. Sci. 58, 1463–1471. https://doi.org/ 10.1002/pol.20200089.
- Wilson, O.R., McDaniel, R.M., Rivera, A.D., and Magenau, A.J.D. (2020). Alkylborane-initiated thiol-ene networks for the synthesis of thick and highly loaded nanocomposites. ACS Appl. Mater. Interfaces 12, 55262–55268. https://doi. org/10.1021/acsami.0c16587.
- Wilson, O.R., Borrelli, D.J., and Magenau, A.J.D. (2022). Simple and rapid adhesion of commodity polymer substrates under ambient conditions using complexed alkylboranes. ACS Omega 7, 28636–28645. https://doi.org/10. 1021/acsomega.2c03740.
- 40. Fairbanks, B.D., Sims, E.A., Anseth, K.S., and Bowman, C.N. (2010). Reaction rates and mechanisms for radical, photoinitated addition

- of thiols to alkynes, and implications for Thiol—Yne photopolymerizations and click reactions. Macromolecules 43, 4113–4119. https://doi.org/10.1021/ma/1002968.
- Hine, J., and Via, F.A. (1972). Kinetics of the formation of imines from isobutyraldehyde and primary aliphatic amines with polar substituents. J. Am. Chem. Soc. 94, 190–194. https://doi.org/10.1021/ja00756a033.
- Chan, J.W., Hoyle, C.E., Lowe, A.B., and Bowman, M. (2010). Nucleophile-initiated thiolmichael reactions: effect of organocatalyst, thiol, and ene. Macromolecules 43, 6381–6388. https://doi.org/10.1021/ma101069c.
- Ahn, D., Wier, K.A., Mitchell, T.P., and Olney, P.A. (2015). Applications of fast, facile, radiation-free radical polymerization techniques enabled by room temperature alkylborane chemistry. ACS Appl. Mater. Interfaces 7, 23902–23911. https://doi.org/10. 1021/acsami.5b05943.
- Fedorov, A.V., Ermoshkin, A.A., Mejiritski, A., and Neckers, D.C. (2007). New method to reduce oxygen surface inhibition by photorelease of boranes from borane/amine complexes. Macromolecules 40, 3554–3560. https://doi.org/10.1021/ma062025+.
- Schechtel, E., Yan, Y., Xu, X., Cang, Y., Tremel, W., Wang, Z., Li, B., and Fytas, G. (2017). Elastic modulus and thermal conductivity of thiolene/ TiO2 nanocomposites. J. Phys. Chem. C Nanomater. Interfaces 121, 25568–25575. https://doi.org/10.1021/acs.jpcc.7b08425.
- 46. Christensen, R.M. (2005). A concentrated suspension model. In Mechanics of Composite Materials (Dover Publications).
- Watanabe, K., Miwa, E., Asai, F., Seki, T., Urayama, K., Nakatani, T., Fujinami, S., Hoshino, T., Takata, M., Liu, C., et al. (2020). Highly transparent and tough filler composite elastomer inspired by the cornea. ACS Mater. Lett. 2, 325–330. https://doi.org/10.1021/ acsmaterialslett.9b00520.
- Mermet-Guyennet, M.R.B., Gianfelice de Castro, J., Varol, H.S., Habibi, M., Hosseinkhani, B., Martzel, N., Sprik, R., Denn, M.M., Zaccone, A., Parekh, S.H., and Bonn, D. (2015). Size-dependent reinforcement of composite rubbers. Polymer 73, 170–173. https://doi.org/10.1016/j.polymer.2015. 07.041.